Isotropic Design of Spatial Parallel Manipulators

A. Fattah

Department of Mechanical Engineering
University of Delaware
Newark, DE 19716, USA
fattah@me.udel.edu

A.M. Hasan Ghasemi

Department of Mechanical Engineering
Isfahan University of Technology
Isfahan, Iran

Abstract

In this paper, we study the isotropic design of two types of spatial parallel manipulators: a three-degrees-of-freedom manipulator and the Stewart–Gough platform. The isotropic conditions for Jacobian matrices, which relate the input joint velocity and output Cartesian velocity, are determined separately using a pure symbolic method. Thereafter, upon determining the isotropic conditions for both manipulators, the variation of the kinematic condition index is studied with respect to the motion of the moving platform to show how far the manipulator is from being isotropic. Finally, the isotropic conditions are obtained numerically for both manipulators.

KEY WORDS—parallel manipulators, isotropic design, Jacobian matrix

1. Introduction

Parallel manipulation has been the subject of study of many robotic researchers during the last two decades. Accuracy, rigidity, high speed, and high load-to-weight ratio are the main merits of parallel manipulators as compared with serial manipulators. The optimal design of parallel manipulators is one of the important issues in research (Gallant and Boudreau 2002, Carretero et al. 2000; Huang and Whitehouse 1998; Gosselin, St-Pierre, and Gagné 1996). The isotropic design of a robot aims at ideal kinematic and dynamic performance of the robot. There are some research works on the isotropic design of parallel manipulators (Baron and Bernier 2001; Zanganeh and Angeles 1997; Chablat, Wenger, and Angeles 1998; Mohammadi Daniali and Zsombor-Murray 1994; Gosselin and Lavoie 1993; Gosselin and Angeles 1988). Zanganeh and Angeles (1997) have worked on the Jacobian matrices of parallel manipulators. They have studied the isotropic design of a Stewart–Gough platform for a special case of vertical translational motion of the moving platform. Chablat, Wenger, and Angeles (1998) have considered a class of two-degrees-of-freedom (2-DoF) robots that are composed of a five bar mechanism in a closed loop. They have determined curves with the same condition number. Then they have added a rotational DoF to the system and obtained the surfaces with the same condition number for the 3-DoF mechanism. Mohammadi and Zsombor-Murray (1994) have worked on the isotropic design of two special cases of planar parallel manipulators. Gosselin and Angeles (1988) have considered the kinematic design of planar parallel manipulators using four criteria: (i) the existence of workspace in any direction; (ii) maximum workspace; (iii) similarity; (iv) isotropic design. To the best of our knowledge, the work on the isotropic design of parallel manipulators has considered only the planar or spatial cases with only the translational motion of the moving platform.

Isotropicity of a robotic manipulator is related to condition number of its Jacobian matrix, which can be obtained using singular values. We call a robotic manipulator completely isotropic if its Jacobian matrix is isotropic, i.e., the condition number of its Jacobian matrix is one. An isotropic manipulator is superior in kinematic accuracy and does not have singular configurations.

The joint rates and Cartesian velocities of the moving platform of a manipulator are related by means of two Jacobian matrices: (i) the direct or forward kinematic Jacobian matrix, $\mathbf{A}$; (ii) the inverse kinematic Jacobian matrix, $\mathbf{B}$. The isotropic conditions apply to either both Jacobian matrices or one Jacobian matrix, i.e., $\mathbf{G} = \mathbf{B}^{-1}\mathbf{A}$ to determine the isotropic design of parallel manipulators.

In this paper, our main aim is to answer the question: how does the kinematic condition index (KCI) vary with the motion of the moving platform of the manipulator to show closeness

The International Journal of Robotics Research
Vol. 21, No. 9, September 2002, pp. 811-824,

to isotropicity. We study the isotropic design of two types of parallel manipulators: a 3-DoF spatial parallel manipulator and a Stewart–Gough platform (Stewart 1965). The kinematic parameters and constraint equations for both manipulators are studied first. Then, the isotropic conditions for both Jacobian matrices of the manipulators are determined separately using symbolic computation. The moving platform has both orientational and translational motion for the 3-DoF manipulator and translational motion in three directions for the Stewart–Gough platform. Finally, the isotropic configurations for both manipulators are obtained numerically using the isotropic conditions for the Jacobian matrix **G** of each manipulator.

2. Parallel Manipulators

2.1 The 3-DoF Spatial Parallel Manipulator

The parallel manipulator at hand consists of a moving platform (MP) and a base platform (BP) that are connected to each other by means of four legs, as shown in Figure 1.

Each leg contains two links coupled by a prismatic joint. The central leg is connected to the MP by a universal joint and fixed to the BP. The other three legs are connected to the MP by spherical joints and to the BP by universal joints. The frames *XYZ* and *xyz* are inertial and moving frames attached to the BP and MP at points O and O_M, respectively. The system has 3-DoF and three linear actuators are connected to three circumferential legs. Hence the MP has three motions: translation along the Z-axis (heave), rotation about the y-axis (pitch) and rotation about the x-axis (roll). Upon obtaining the kinematic constraint equations and the time differentiation of the equations thus obtained, we can obtain the relation between input or joint velocity, $\dot{\mathbf{q}}$, and the output or Cartesian velocity, **t**, as follows

$$\mathbf{A}\mathbf{t} = \mathbf{B}\dot{\mathbf{q}}, \tag{1}$$

where

$$\dot{\mathbf{q}} = \begin{bmatrix} \dot{\mathbf{q}}_1 & \dot{\mathbf{q}}_2 & \dot{\mathbf{q}}_3 \end{bmatrix}^{\mathrm{T}} \tag{2a}$$

$$\mathbf{t} = \begin{bmatrix} \dot{\varphi} & \dot{\psi} & \dot{h} \end{bmatrix}^{\mathrm{T}}. \tag{2b}$$

Here, φ, ψ, and h are the roll, pitch, and heave of the MP, and q_1, q_2 and q_3 are the lengths of the legs. Moreover, the 3×3 matrices **A** and **B** are

$$\mathbf{A} = \begin{bmatrix} a_{11} & a_{12} & a_{13} \\ a_{21} & a_{22} & a_{23} \\ a_{31} & a_{32} & a_{33} \end{bmatrix} \tag{3a}$$

$$\mathbf{B} = \begin{bmatrix} q_1 & 0 & 0 \\ 0 & q_2 & 0 \\ 0 & 0 & q_3 \end{bmatrix}, \tag{3b}$$

where the elements of **A** are defined as

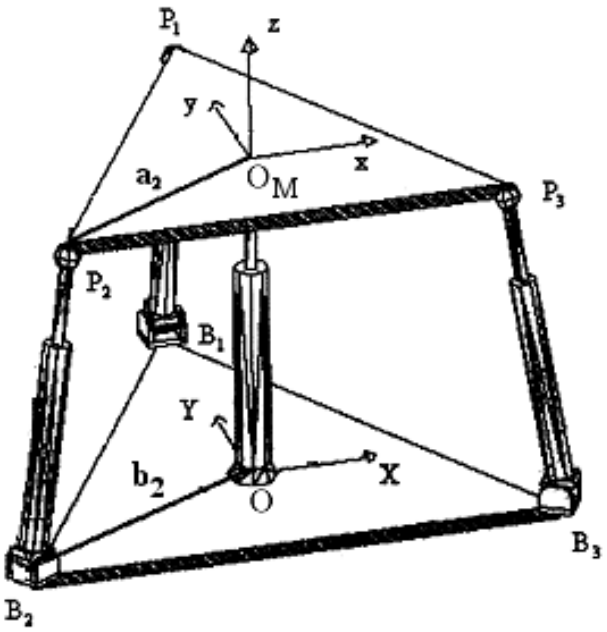

Fig. 1. The 3-DoF spatial parallel manipulator.

$$a_{11} = r_m(r_b \sin\varphi + h\cos\varphi) \tag{4a}$$

$$a_{12} = 0 \tag{4b}$$

$$a_{13} = h + r_m \sin\varphi \tag{4c}$$

$$a_{21} = -\sqrt{3}/4 r_m r_b \cos\varphi \sin\psi + 1/4 r_m r_b \sin\varphi - \sqrt{3}/2 r_m h \sin\varphi \sin\psi - 1/2 r_m h \cos\varphi \tag{4d}$$

$$a_{22} = 3/4 r_m r_b \sin\psi - \sqrt{3}/4 r_m r_b \sin\varphi \cos\psi + \sqrt{3}/2 r_m h \cos\varphi \sin\psi \tag{4e}$$

$$a_{23} = h + \sqrt{3}/2 r_m \cos\varphi \sin\psi - 1/2 r_m \sin\varphi \tag{4f}$$

$$a_{31} = \sqrt{3}/4 r_m r_b \cos\varphi \sin\psi + 1/4 r_m r_b \sin\varphi + \sqrt{3}/2 r_m h \sin\varphi \sin\psi - 1/2 r_m h \cos\varphi \tag{4g}$$

$$a_{32} = 3/4 r_m r_b \sin\psi + \sqrt{3}/4 r_m r_b \sin\varphi \cos\psi - \sqrt{3}/2 r_m h \cos\varphi \cos\psi \tag{4h}$$

$$a_{33} = h - \sqrt{3}/2 r_m \cos\varphi \sin\psi - 1/2 r_m \sin\varphi. \tag{4i}$$

Here r_b and r_m are the radii of the circumferential circles of the BP and MP, as shown in Figure 2. It is assumed that both the BP and the MP are equilateral triangles. The complete

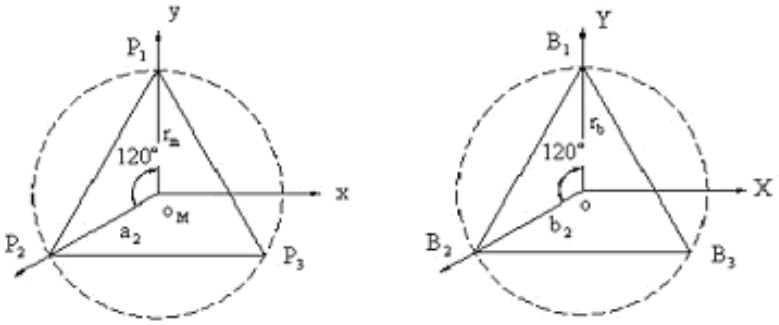

Fig. 2. MP and BP shapes of the 3-DoF parallel manipulator.

derivation of eq. (1) can be obtained in Fattah and Oghbaei (2000).

2.2 Stewart–Gough Platform

This mechanism is composed of a BP and MP, which are connected to each other by six legs, as shown in Figure 3.

Each leg connects to the MP by a spherical joint and to the BP by a universal joint. The legs contain two links coupled by a prismatic joint. As shown in Figure 3, the centroids of the BP and the MP are O and O_M, respectively. The reference frame $\mathcal{B}$ at O is assigned such that the Y-axis is parallel to B_1B_2 and the Z-axis is perpendicular to the BP, and the frame $\mathcal{M}$ is also assigned at O_M with the y-axis parallel to P_1P_2 and the z-axis perpendicular to the MP.

Upon definition of r_b and r_m as the radii of circumferential circles of the BP and MP, depicted in Figure 4, the position vectors of vertices of the base platform with respect to frame $\mathcal{B}$, i.e., $\mathbf{b}_i = \overrightarrow{OB_i}(i = 1, \ldots, 6)$ and the position vectors of vertices of the moving platform with respect to frame $\mathcal{M}$, i.e., $\mathbf{a}_i = \overrightarrow{O_MP_i}(i = 1, \ldots, 6)$ are written as

$$\mathbf{a}_1 = \begin{bmatrix} r_m \cos\left(\frac{\varphi_m}{2}\right) & -r_m \sin\left(\frac{\varphi_m}{2}\right) & 0 \end{bmatrix}^{\mathrm{T}} \tag{5}$$

$$\mathbf{a}_2 = \begin{bmatrix} r_m \cos\left(\frac{\varphi_m}{2}\right) & r_m \sin\left(\frac{\varphi_m}{2}\right) & 0 \end{bmatrix}^{\mathrm{T}} \tag{6}$$

$$\mathbf{a}_3 = \mathbf{Q}_1\mathbf{a}_1 \tag{7}$$

$$\mathbf{a}_4 = \mathbf{Q}_1\mathbf{a}_2 \tag{8}$$

$$\mathbf{a}_5 = \mathbf{Q}_2\mathbf{a}_1 \tag{9}$$

$$\mathbf{a}_6 = \mathbf{Q}_2\mathbf{a}_2 \tag{10}$$

$$\mathbf{b}_1 = \begin{bmatrix} r_b \cos\left(\frac{\varphi_b}{2}\right) & -r_b \sin\left(\frac{\varphi_b}{2}\right) & 0 \end{bmatrix}^{\mathrm{T}} \tag{11}$$

$$\mathbf{b}_2 = \begin{bmatrix} r_b \cos\left(\frac{\varphi_b}{2}\right) & r_b \sin\left(\frac{\varphi_b}{2}\right) & 0 \end{bmatrix}^{\mathrm{T}} \tag{12}$$

$$\mathbf{b}_3 = \mathbf{Q}_1\mathbf{b}_1 \tag{13}$$

$$\mathbf{b}_4 = \mathbf{Q}_1\mathbf{b}_2 \tag{14}$$

$$\mathbf{b}_5 = \mathbf{Q}_2\mathbf{b}_1 \tag{15}$$

$$\mathbf{b}_6 = \mathbf{Q}_2\mathbf{b}_2, \tag{16}$$

where φ_b and φ_m are the separation angles of the BP and MP, which are shown in Figure 4.

Moreover, $\mathbf{Q}_1$ and $\mathbf{Q}_2$ are rotation matrices about the Z-axis through angles 120° and 240°, respectively, as

$$\mathbf{Q}_1 = \begin{bmatrix} \cos(2\pi/3) & -\sin(2\pi/3) & 0 \\ \sin(2\pi/3) & \cos(2\pi/3) & 0 \\ 0 & 0 & 1 \end{bmatrix} \tag{17a}$$

$$\mathbf{Q}_2 = \begin{bmatrix} \cos(4\pi/3) & -\sin(4\pi/3) & 0 \\ \sin(4\pi/3) & \cos(4\pi/3) & 0 \\ 0 & 0 & 1 \end{bmatrix} \tag{17b}$$

The rotation matrix for the general motion, roll–pitch–yaw, of the MP, i.e., the fixed Euler angles φ, ψ and θ, can be written as

$$\mathbf{R} = \begin{bmatrix} \mathrm{c}\psi\mathrm{c}\theta & -\mathrm{c}\psi\sin\theta & \mathrm{s}\psi \\ \mathrm{s}\varphi\mathrm{s}\psi\mathrm{c}\theta + \mathrm{c}\varphi\mathrm{s}\theta & -\mathrm{s}\varphi\mathrm{s}\psi\mathrm{s}\theta + \mathrm{c}\varphi\mathrm{c}\theta & -\mathrm{s}\varphi\mathrm{c}\psi \\ -\mathrm{c}\varphi\mathrm{s}\psi\mathrm{c}\theta + \mathrm{s}\varphi\mathrm{s}\theta & \mathrm{c}\varphi\mathrm{s}\psi\mathrm{s}\theta + \mathrm{s}\varphi\mathrm{c}\theta & \mathrm{c}\varphi\mathrm{c}\psi \end{bmatrix}, \tag{18}$$

where c and s denote cos and sin, respectively.

Upon expressing the kinematic constraint equations and differentiating the equations thus obtained with respect to time, we obtain the kinematic relations governing the problem as follows

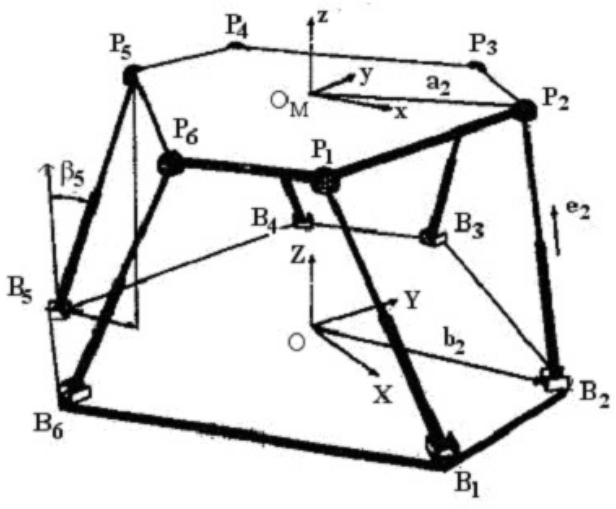

Fig. 3. Stewart–Gough platform.

$$\mathbf{At} = \mathbf{B}\dot{\mathbf{q}} \tag{19}$$

$$\dot{\mathbf{q}} = \begin{bmatrix} \dot{q}_1 & \dot{q}_2 & \dot{q}_3 & \dot{q}_4 & \dot{q}_5 & \dot{q}_6 \end{bmatrix}^{\mathrm{T}} \tag{20}$$

$$\mathbf{t} = \begin{bmatrix} \boldsymbol{\omega}_{MP}^{\mathrm{T}} & \dot{\mathbf{p}}^{\mathrm{T}} \end{bmatrix}^{\mathrm{T}} \tag{21}$$

$$\mathbf{A} = \begin{bmatrix} (\mathbf{a}_1 \times \mathbf{l}_1)^{\mathrm{T}} & \mathbf{l}_1^{\mathrm{T}} \\ (\mathbf{a}_2 \times \mathbf{l}_2)^{\mathrm{T}} & \mathbf{l}_2^{\mathrm{T}} \\ (\mathbf{a}_3 \times \mathbf{l}_3)^{\mathrm{T}} & \mathbf{l}_3^{\mathrm{T}} \\ (\mathbf{a}_4 \times \mathbf{l}_4)^{\mathrm{T}} & \mathbf{l}_4^{\mathrm{T}} \\ (\mathbf{a}_5 \times \mathbf{l}_5)^{\mathrm{T}} & \mathbf{l}_5^{\mathrm{T}} \\ (\mathbf{a}_6 \times \mathbf{l}_6)^{\mathrm{T}} & \mathbf{l}_6^{\mathrm{T}} \end{bmatrix} \tag{22}$$

$$\mathbf{B} = \begin{bmatrix} q_1 & 0 & 0 & 0 & 0 & 0 \\ 0 & q_2 & 0 & 0 & 0 & 0 \\ 0 & 0 & q_3 & 0 & 0 & 0 \\ 0 & 0 & 0 & q_4 & 0 & 0 \\ 0 & 0 & 0 & 0 & q_5 & 0 \\ 0 & 0 & 0 & 0 & 0 & q_6 \end{bmatrix} \tag{23}$$

where $\mathbf{A}$ and $\mathbf{B}$ are Jacobian matrices. $\dot{\mathbf{q}}$ is the joint velocity vector and $\mathbf{t}$ is the twist vector of the MP. $\boldsymbol{\omega}_{MP}$ and $\dot{\mathbf{p}}$ in eq. (21) are the angular and linear velocity vectors of the centroid of the MP with respect to the reference frame, respectively. Moreover, $\mathbf{l}_i$ is the leg vector and can be written as

$$\mathbf{l}_i = \mathbf{p} + \mathbf{R}\mathbf{a}_i - \mathbf{b}_i \quad (i, 1, \ldots, 6) \tag{24}$$

$$\mathbf{l}_i = q_i \mathbf{e}_i \quad (i, 1, \ldots, 6), \tag{25}$$

where $\mathbf{p}$ is the position vector of the centriod of the MP with respect to O, i.e., $\mathbf{p} = \overrightarrow{\mathrm{OO}}_{\mathrm{M}}$ and $\mathbf{e}_i$ is the unit vector along leg i.

3. Isotropic Design of Parallel Manipulators

There are two Jacobian matrices relating the joint and Cartesian velocities, as expressed in eqs. (3) for the 3-DoF manipulator and in eqs. (22) and (23) for the Stewart–Gough platform, namely the forward kinematic matrix $\mathbf{A}$ and the inverse kinematic matrix $\mathbf{B}$ (Gosselin and Angeles 1988). The conditions for isotropy should apply to both matrices as described in Gosselin and Angeles (1988). These two Jacobian matrices are isotropic if they are proportional to an identity matrix (Angeles and Lopez-Cajun 1992; Angeles 1997), namely,

$$\mathbf{A}^{\mathrm{T}}\mathbf{A} = \sigma^2\mathbf{I} \tag{26}$$

$$\mathbf{B}^{\mathrm{T}}\mathbf{B} = \tau^2\mathbf{I}, \tag{27}$$

where $\mathbf{I}$ is an identity matrix and σ and τ are two scalars. In other words, an isotropic matrix has identical singular values with a condition number of one. The isotropic conditions for the 3-DoF manipulator with a roll, pitch and heave motion of the MP and the isotropic conditions for the Stewart–Gough platform for a general translational motion of the MP are studied in Sections 3.1 and 3.2 using pure symbolic computation on the isotropic conditions for both Jacobian matrices $\mathbf{A}$ and $\mathbf{B}$.

Nevertheless, isotropic conditions for parallel manipulators can also be determined by multiplying both sides of eq. (1) or eq. (19) by $\mathbf{B}^{-1}$, to obtain

$$\dot{\mathbf{q}} = \mathbf{B}^{-1}\mathbf{At}. \tag{28}$$

If matrix $\mathbf{G}$ is defined as

$$\mathbf{G} = \mathbf{B}^{-1}\mathbf{A}, \tag{29}$$

the input and output velocities can be related only by one Jacobian matrix

$$\dot{\mathbf{q}} = \mathbf{B}^{-1}\mathbf{At} = \mathbf{Gt}. \tag{30}$$

Here, the isotropic conditions apply to the Jacobian matrix $\mathbf{G}$ instead of both matrices $\mathbf{A}$ and $\mathbf{B}$. The isotropic configurations for both manipulators are obtained numerically upon applying the isotropic conditions to the Jacobian matrix $\mathbf{G}$ in Section 4.

3.1 Isotropy Design of the 3-DoF Manipulator

3.1.1 Isotropy Conditions of $\mathbf{A}$

We determine the isotropy conditions for matrix $\mathbf{A}$ first. To compare the singular values of a matrix, the elements of this matrix should have the same units. From eq. (3a), the elements of the first and second columns of matrix $\mathbf{A}$ have the units of (length)^2. The third column has the unit of length. The characteristic length of the manipulator, i.e., L, is used to homogenize the elements of Jacobian matrix so that the condition number is non-dimensional (Angeles 1997).

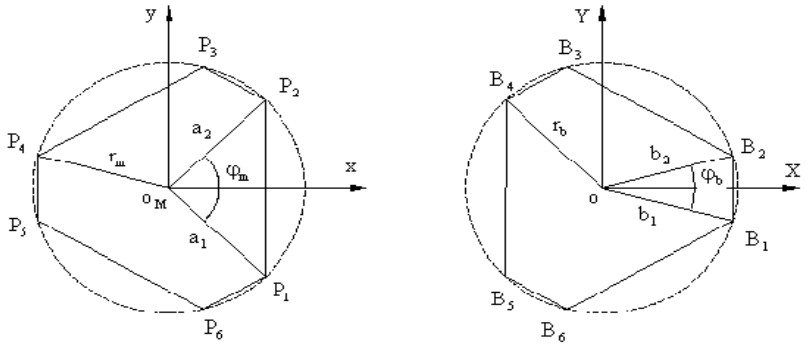

Fig. 4. MP and BP shapes of the Stewart–Gough platform.

Therefore, the first two columns are divided by characteristic length L and the matrix $\mathbf{A}$ is divided into two submatrices $\mathbf{F}_p$ and $\mathbf{F}_o$ as

$$\mathbf{A} = \begin{bmatrix} \frac{1}{L}\mathbf{F}_p & \mathbf{F}_o \end{bmatrix}, \tag{31}$$

where $\mathbf{F}_p$ is 3×2 matrix and $\mathbf{F}_o$ is a three-dimensional vector.

Upon substitution of eq. (31) into eq. (26), i.e., the isotropic condition for Jacobian matrix $\mathbf{A}$ requires

$$\mathbf{A}^{\mathrm{T}}\mathbf{A} = \begin{bmatrix} \frac{1}{L^2}\mathbf{F}_p^{\mathrm{T}}\mathbf{F}_p & \frac{1}{L}\mathbf{F}_p^{\mathrm{T}}\mathbf{F}_o \\ \frac{1}{L}\mathbf{F}_o^{\mathrm{T}}\mathbf{F}_p & \mathbf{F}_o^{\mathrm{T}}\mathbf{F}_o \end{bmatrix} = \begin{bmatrix} \sigma^2\mathbf{I}_2 & \mathbf{0} \\ \mathbf{0}^{\mathrm{T}} & \sigma^2 \end{bmatrix} \tag{32}$$

where $\mathbf{I}_2$ is a 2×2 identity matrix and $\mathbf{0}$ is a two-dimensional zero vector. Equation (32) implies that

$$\frac{1}{L^2}\mathbf{F}_p^{\mathrm{T}}\mathbf{F}_p = \sigma^2\mathbf{I}_2 \tag{33a}$$

$$\mathbf{F}_o^{\mathrm{T}}\mathbf{F}_o = \sigma^2 \tag{33b}$$

$$\frac{1}{L}\mathbf{F}_p^{\mathrm{T}}\mathbf{F}_o = \mathbf{0}. \tag{33c}$$

Comparing the traces of both sides of eqs. (33a) and (33b) leads to

$$L^2 = \frac{\mathrm{tr}(\mathbf{F}_p^{\mathrm{T}}\mathbf{F}_p)}{2(\mathbf{F}_o^{\mathrm{T}}\mathbf{F}_o)}. \tag{34}$$

Upon substitution of the elements of matrices $\mathbf{F}_p$ and $\mathbf{F}_o$ from eqs. (4), we obtain

$$\frac{1}{L^2}\mathbf{F}_p^{\mathrm{T}}\mathbf{F}_p = \frac{1}{L^2}\begin{bmatrix} K_1 & K_2 \\ K_2 & K_3 \end{bmatrix} = \begin{bmatrix} \sigma^2 & 0 \\ 0 & \sigma^2 \end{bmatrix} \tag{35a}$$

$$\mathbf{F}_o^{\mathrm{T}}\mathbf{F}_o = K_4 = \sigma^2 \tag{35b}$$

$$\frac{1}{L}\mathbf{F}_p^{\mathrm{T}}\mathbf{F}_o = \frac{1}{L}\begin{bmatrix} K_5 \\ K_6 \end{bmatrix} = \begin{bmatrix} 0 \\ 0 \end{bmatrix} \tag{35c}$$

where $K_i (i = 1, \ldots 6)$ are defined as

$$\begin{aligned} K_1 = {} & 3/8 r_m^2 (3 r_b^2 \sin^2\varphi + 4 r_b h \sin\varphi\cos\varphi \\ & + 4h^2\cos^2\varphi + r_b^2\cos^2\varphi\sin^2\psi \\ & + 4 r_b h \sin\varphi\cos\varphi\sin^2\psi + 4h^2\sin^2\varphi\sin^2\psi) \end{aligned} \tag{36a}$$

$$\begin{aligned} K_2 = {} & -3/8 r_m^2 \sin\psi (2h\cos\varphi - r_b\sin\varphi) \\ & (2h\sin\varphi\cos\psi + r_b\cos\varphi\cos\psi + r_b) \end{aligned} \tag{36b}$$

$$\begin{aligned} K_3 = {} & 3/8 r_m^2 (3 r_b^2 \sin^2\psi + r_b^2\sin^2\varphi\cos^2\psi \\ & - 4 r_b h \sin\varphi\cos\varphi\cos^2\psi + 4h^2\cos^2\varphi\cos^2\psi) \end{aligned} \tag{36c}$$

$$K_4 = 3h^2 + 3/2 r_m^2 \sin^2\varphi + 3/2 r_m^2 \cos^2\varphi\sin^2\psi \tag{36d}$$

$$\begin{aligned} K_5 = {} & 3/4 r_m (2 r_m h \sin\varphi\cos\varphi\cos^2\psi \\ & + 2 r_b h \sin\varphi + r_m r_b \sin^2\varphi - r_m r_b \cos^2\varphi\sin^2\psi) \end{aligned} \tag{36e}$$

$$\begin{aligned} K_6 = {} & 3/4 r_m \sin\psi (2 r_m h \cos^2\varphi\cos\psi + 2 r_b h \\ & - r_m r_b \sin\varphi - r_m r_b \sin\varphi\cos\varphi\cos\psi). \end{aligned} \tag{36f}$$

Eqs. (35) lead to the following conditions

$$K_2 = K_5 = K_6 = 0 \tag{37a}$$

$$\frac{1}{L^2}K_1 = \frac{1}{L^2}K_3 = K_4 = \sigma^2. \tag{37b}$$

The above equations have only one solution when the matrix $\mathbf{A}$ is isotropic. In this case, matrix $\mathbf{A}^{\mathrm{T}}\mathbf{A}$ can be written as a diagonal matrix with identical diagonal elements. Upon substitution of eqs. (36) into eqs. (37) and simplifying the result thus obtained, the configuration of the MP for the isotropy condition of Jacobian matrix $\mathbf{A}$ is obtained as

$$\psi = 0, \quad \varphi = -\cos^{-1}(r_b/r_m), \quad h = \frac{\sqrt{r_m^2 - r_b^2}}{4}. \tag{38}$$

By substituting eq. (38) into eqs. (35a) and (35b), we find

$$\mathbf{F}_p^{\mathrm{T}}\mathbf{F}_p = \begin{bmatrix} \frac{27}{32}r_b^2(r_m^2 - r_b^2) & 0 \\ 0 & \frac{27}{32}r_b^2(r_m^2 - r_b^2) \end{bmatrix} \tag{39a}$$

$$\mathbf{F}_o^{\mathrm{T}}\mathbf{F}_o = \left[\frac{27}{16}(r_m^2 - r_b^2)\right]. \tag{39b}$$

Moreover the characteristic length for the isotropic condition is obtained by inserting eq. (38) into eq. (34) as

$$L = \frac{\sqrt{2}}{2}r_b. \tag{40}$$

Therefore, matrix $\mathbf{A}^{\mathrm{T}}\mathbf{A}$ for the isotropy condition of matrix $\mathbf{A}$ can be determined by substituting eqs. (39) and (40) into eq. (32) as

$$\mathbf{A}^{\mathrm{T}}\mathbf{A} = \begin{bmatrix} \frac{27}{32}(r_m^2 - r_b^2) & 0 & 0 \\ 0 & \frac{27}{32}(r_m^2 - r_b^2) & 0 \\ 0 & 0 & \frac{27}{32}(r_m^2 - r_b^2) \end{bmatrix}. \tag{41}$$

3.1.2 Isotropy Condition of **B**

Next we determine the isotropy condition for matrix $\mathbf{B}$ using eq. (3b). The inverse kinematic matrix $\mathbf{B}$ is a diagonal matrix. Hence, the isotropy condition for this matrix is to have identical diagonal elements for $\mathbf{B}$, namely

$$q_1 = q_2 = q_3. \tag{42}$$

The above equation dictates that isotropy for matrix $\mathbf{B}$ occurs when the length of the legs are identical. This occurs when the pitch and roll angles of the MP are zero.

It may be noted that when $\mathbf{A}$ is isotropic, the other Jacobian matrix $\mathbf{B}$ may not be isotropic and vice versa. Here, we study the KCI of the matrices $\mathbf{A}$ and $\mathbf{B}$ when the other matrix is isotropic.

3.1.3 Variations of KCI

The KCI can be defined as

$$\mathrm{KCI}(\mathbf{J}) = \frac{1}{k(\mathbf{J})} \times 100\%, \tag{43}$$

where $k(\mathbf{J})$ is the condition number of a Jacobian matrix $\mathbf{J}$. A matrix with a KCI of 100% is isotropic while that with a KCI of 0% is singular. Hence it can be inferred that a higher KCI makes a matrix closer to the isotropic condition and a lower KCI makes it closer to singularity.

Using the inverse kinematics of the manipulator at hand, we can easily express the length of each leg in terms of roll, pitch and heave of the manipulator, when the matrix $\mathbf{A}$ is isotropic, as

$$q_1 = \frac{3}{4}r_b\sqrt{k_n^2 - 1} \tag{44a}$$

$$q_2 = q_3 = \frac{1}{4}r_b\sqrt{21k_n^2 - 24k_n + 3}, \tag{44b}$$

where $k_n = \frac{r_m}{r_b}$. It is readily known from eq. (38) that $k_n \geq 1$ to satisfy the equations. The radii r_m and r_b are defined in Figure 2.

Thus, the KCI of matrix $\mathbf{B}$ when $\mathbf{A}$ is in the isotropic condition is given as

$$\mathrm{KCI}(\mathbf{B}) = \sqrt{\frac{3k_n^2 - 3}{7k_n^2 - 8k_n + 1}}. \tag{45}$$

The variation of KCI ($\mathbf{B}$) with respect to k_n is depicted in Figure 5. As shown in Figure 5, higher k_n results in a lower KCI of matrix $\mathbf{B}$.

The configuration of the manipulator at hand when matrix $\mathbf{A}$ is isotropic is shown in Figure 6. As shown, the isotropic configuration is not physically realizable.

To alleviate this, the solution should be modified. To this end, the height h in eq. (38) is changed and its variation is determined on KCI($\mathbf{A}$) and KCI($\mathbf{B}$).

If we substitute k_h instead of the coefficient 1/4 in eq. (38), we obtain

$$h = k_n\sqrt{(r_m^2 - r_b^2)}. \tag{46}$$

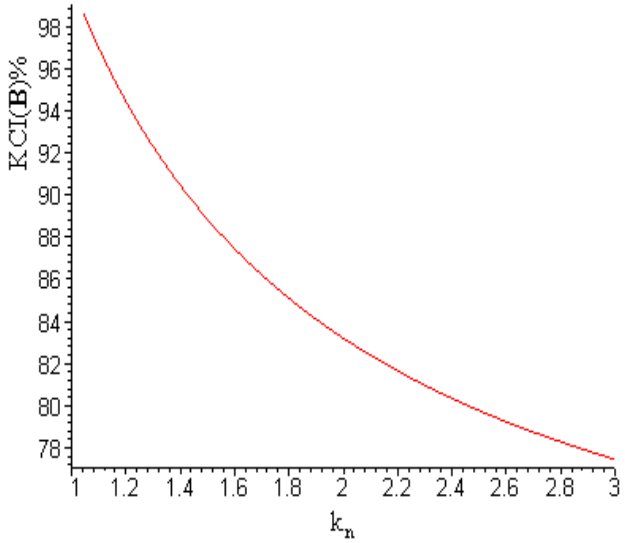

Fig. 5. KCI of matrix $\mathbf{B}$ for the 3-DoF manipulator when matrix $\mathbf{A}$ is isotropic.

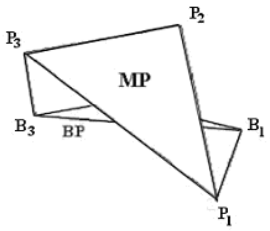

Fig. 6. The configuration of the 3-DoF manipulator when matrix **A** is isotropic.

Upon substitution of h from eq. (46) and φ and ψ from eq. (38) into matrices **A** and **B** and deriving the singular values, the kinematic condition indices for **A** and **B** are written as

$$\mathrm{KCI}(\mathbf{A}) = \frac{2|k_h - 1|}{2k_h + 1} \tag{47a}$$

$$\mathrm{KCI}(\mathbf{B}) = \sqrt{\frac{2(k_n^2 - 1)(k_h - 1)^2}{2k_n^2 - 3k_n + 1 + 2k_h(k_h + 1)(k_n^2 - 1)}}. \tag{47b}$$

As shown from eq. (47a), KCI(**A**) depends only on k_h. The kinematic condition indices for matrices **A** and **B** are shown in Figures 7 and 8, respectively. It can be concluded from these figures that KCI(**A**) and KCI(**B**) increase with increasing k_h. However, eq. (46) shows that increasing k_h causes h to increase. We cannot make k_h too large since there is limitation on h. Hence, to make k_h large without increasing h, the term k_n should be decreased. This means that, at a constant h, on decreasing k_n and increasing k_h, both KCI(**A**) and KCI(**B**) increase.

Finally, the variation of the KCI is studied when the roll and pitch angles of the MP, i.e., φ and ψ, are varied in the range of motion of the mechanism. To this end, φ and ψ are varied about the isotropic solution as follows

$$-\cos^{-1}(r_b/r_m) - 20^\circ \le \varphi \le -\cos^{-1}(r_b/r_m) + 20^\circ$$
$$-20^\circ \le \psi \le 20^\circ. \tag{48}$$

First, the variations of KCI(**A**) and KCI(**B**) with respect to ψ are obtained for different values of k_h and φ. Here, k_h is chosen as 5, 6, 7, 8 and 9 and φ is given as $-\cos^{-1}(r_b/r_m)$, $-\cos^{-1}(r_b/r_m) \pm 5^\circ$, and $-\cos^{-1}(r_b/r_m) \pm 10^\circ$. The curves are shown in Figures 9 and 10 for KCI(**A**) and KCI(**B**), respectively. Next the variations of KCI(**A**) and KCI(**B**) with respect to φ are obtained for different values of k_h and ψ. Likewise, k_h is chosen to be 5, 6, 7, 8 and 9 and ψ is given as 0, $\pm 5^\circ$ and $\pm 10^\circ$. The plots are shown in Figures 11 and 12 for KCI(**A**) and KCI(**B**), respectively. There are five graphs in each subplot of Figures 9–12 where the lowest is for $k_h = 5$ and the highest is for $k_h = 9$.

It can be concluded from Figure 9 that the variation of φ around the isotropic point for φ, i.e., $-\cos^{-1}(r_b/r_m)$, decreases KCI(**A**). Owing to the symmetry of the manipulator about the y-axis, the rate of decrease of KCI(**A**) for angles greater than $\psi = 0^\circ$ is the same as the rate of decrease of KCI(**A**) for angles lower than $\psi = 0^\circ$. The same results can be obtained from Figure 10 for matrix **B**. It may be concluded from Figure 11 that the variation of ψ about the isotropic point for ψ, i.e., $\psi = 0^\circ$, reduced KCI(**A**). Finally, it may be inferred from Figure 12 that increasing the angle φ makes the MP become much more parallel to the BP. This makes length of the legs closer to each other. Therefore, increasing φ causes KCI(**B**) to increase.

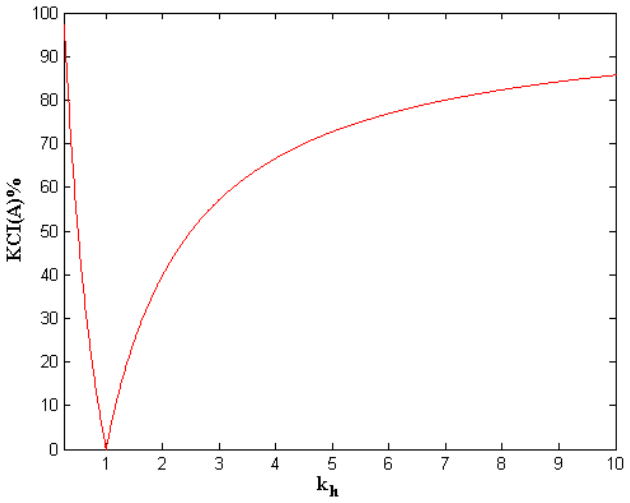

Fig. 7. KCI of matrix **A** of the 3-DoF manipulator.

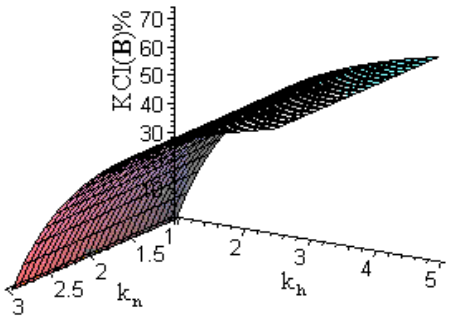

Fig. 8. KCI of matrix **B** of the 3-DoF manipulator.

3.2 Isotropic Design of Stewart–Gough Platform for Translational Motion of the MP

The isotropy condition for matrix **A** is determined first. If the translational motion of the MP is only considered for the Stewart–Gough platform, performing the same procedure as

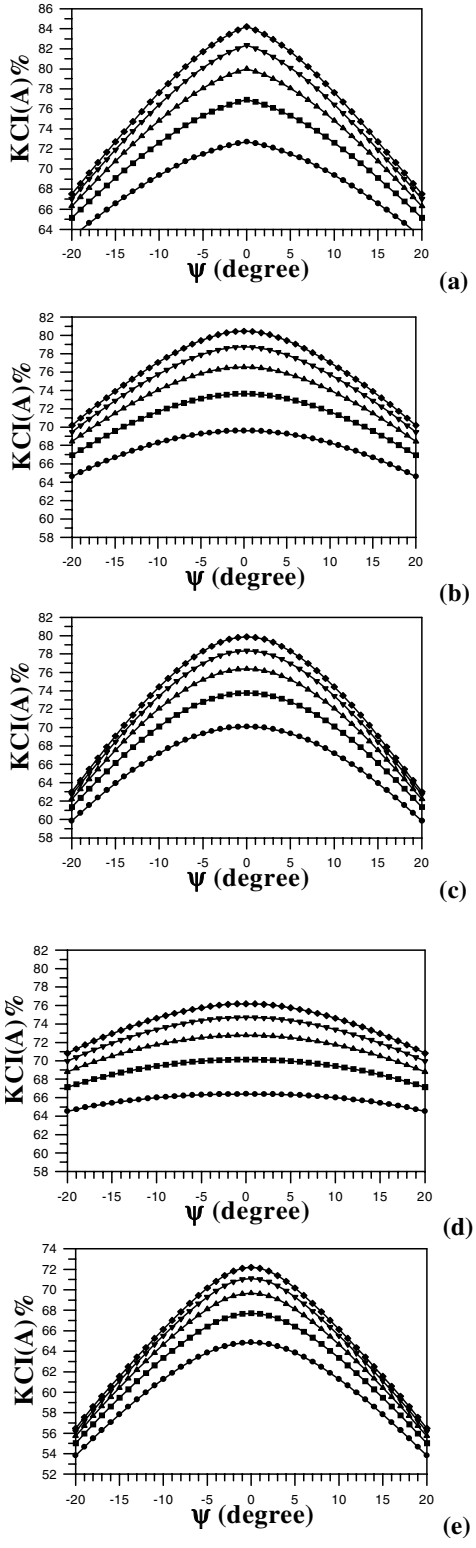

Fig. 9. KCI for matrix **A** versus angles ψ:
(a) $\varphi = -\cos^{-1}(r_b/r_m)$, (b) $\varphi = -\cos^{-1}(r_b/r_m) + 5°$,
(c) $\varphi = -\cos^{-1}(r_b/r_m) - 5°$, (d) $\varphi = -\cos^{-1}(r_b/r_m) + 10°$,
(e) $\varphi = -\cos^{-1}(r_b/r_m) - 10°$.

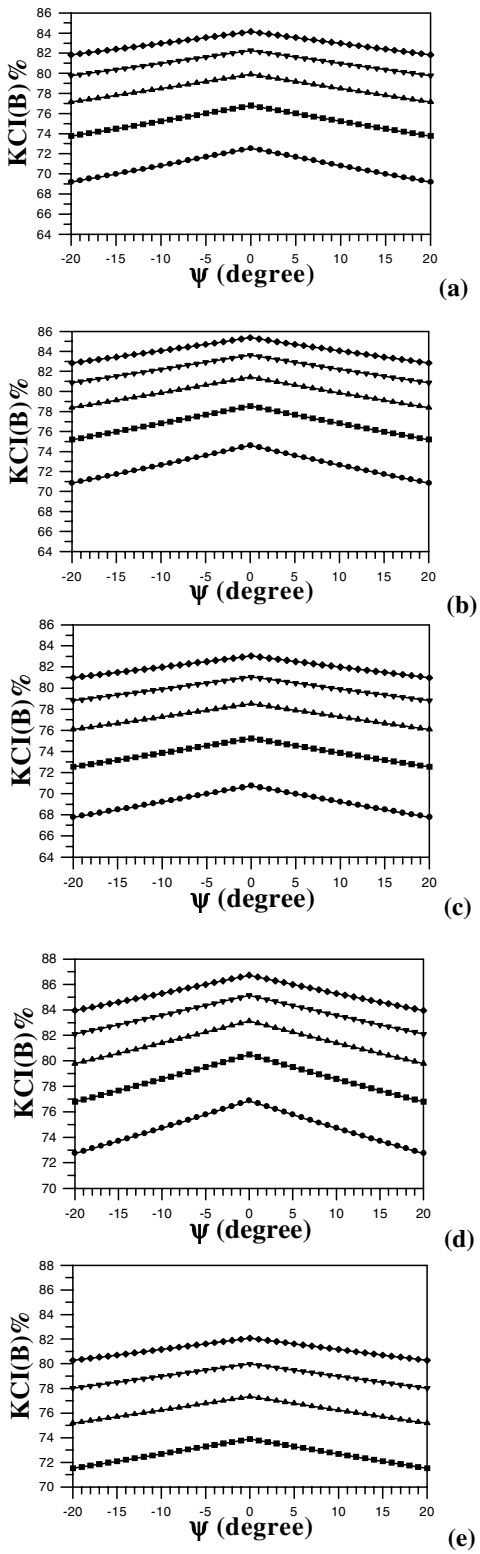

Fig. 10. KCI for matrix **B** versus angles ψ:
(a) $\varphi = -\cos^{-1}(r_b/r_m)$, (b) $\varphi = -\cos^{-1}(r_b/r_m) + 5°$,
(c) $\varphi = -\cos^{-1}(r_b/r_m) - 5°$, (d) $\varphi = -\cos^{-1}(r_b/r_m) + 10°$,
(e) $\varphi = -\cos^{-1}(r_b/r_m) - 10°$.

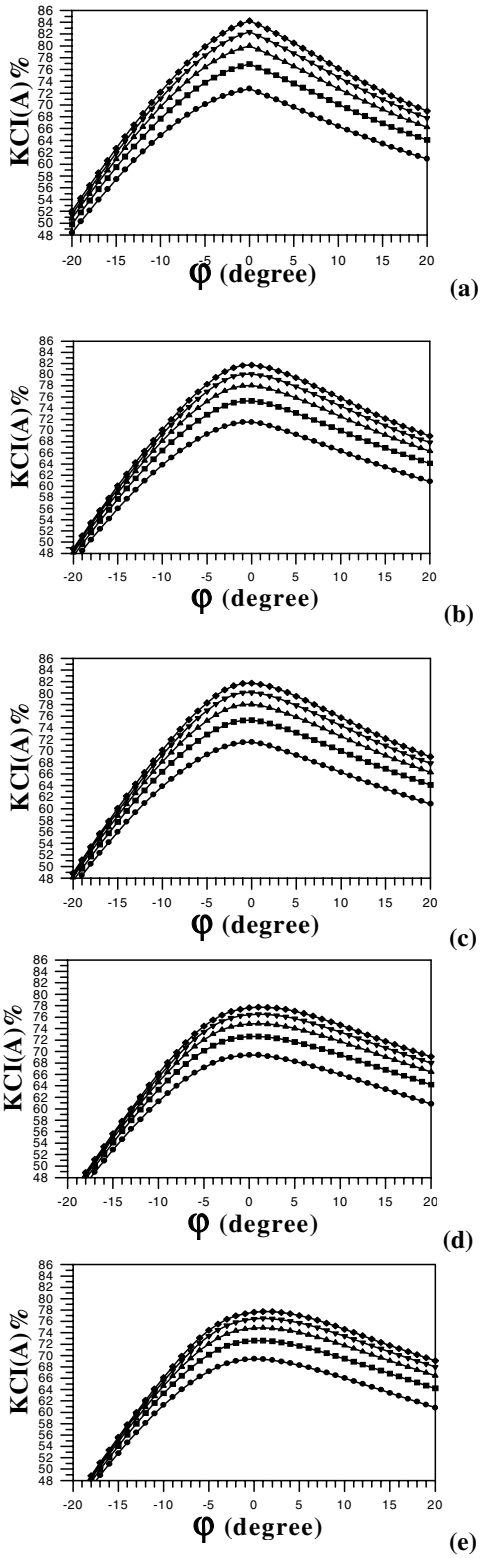

Fig. 11. Kinematic condition index for matrix **A** versus angles ψ: (a) $\psi = -\cos^{-1}(r_b/r_m)$, (b) $\psi = -\cos^{-1}(r_b/r_m) + 5°$, (c) $\psi = -\cos^{-1}(r_b/r_m) - 5°$, (d) $\psi = -\cos^{-1}(r_b/r_m) + 10°$, (e) $\psi = -\cos^{-1}(r_b/r_m) - 10°$.

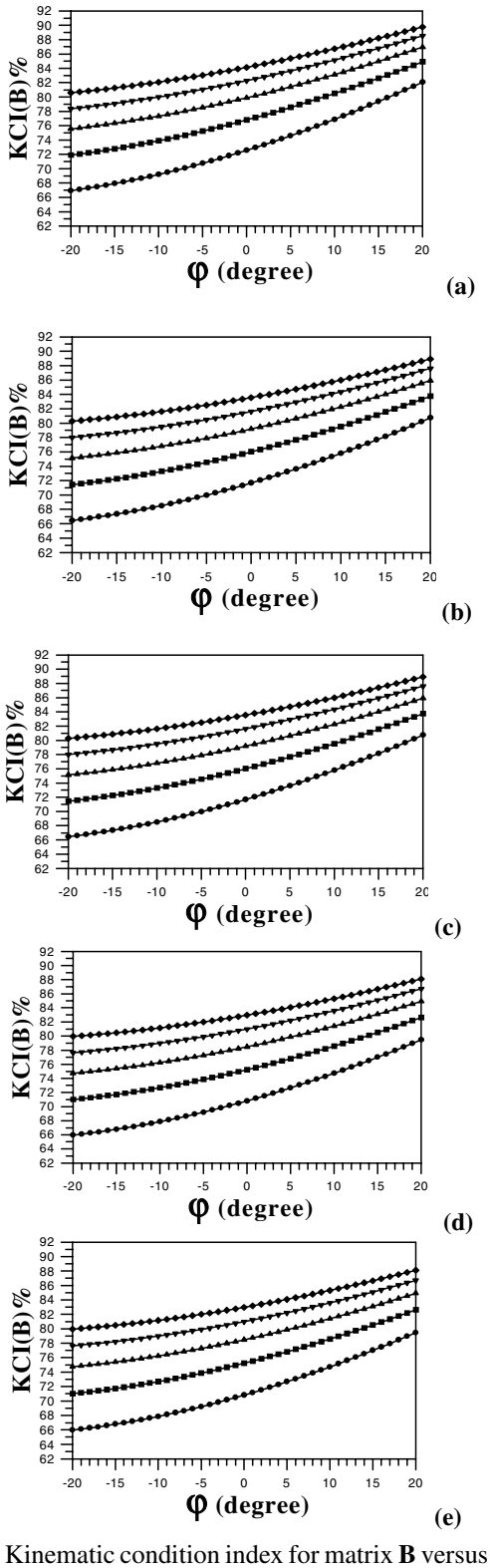

Fig. 12. Kinematic condition index for matrix **B** versus angles ψ: (a) $\psi = -\cos^{-1}(r_b/r_m)$, (b) $\psi = -\cos^{-1}(r_b/r_m) + 5°$, (c) $\psi = -\cos^{-1}(r_b/r_m) - 5°$, (d) $\psi = -\cos^{-1}(r_b/r_m) + 10°$, (e) $\psi = -\cos^{-1}(r_b/r_m) - 10°$.

in Section 3.1.1, $\mathbf{F}_o^{\mathrm{T}}\mathbf{F}_o$, $\mathbf{F}_p^{\mathrm{T}}\mathbf{F}_p$ and $\mathbf{F}_p^{\mathrm{T}}\mathbf{F}_o$ and L can be written in light of eqs. (22) and (23) as

$$\mathbf{F}_o^{\mathrm{T}}\mathbf{F}_o = \begin{bmatrix} 3\eta^2 + 6p_x^2 & 6p_x p_y & 6p_x p_z \\ 6p_x p_y & 3\eta^2 + 6p_y^2 & 6p_y p_z \\ 6p_x p_z & 6p_y p_z & 6p_z^2 \end{bmatrix} \tag{49}$$

$$\mathbf{F}_p^{\mathrm{T}}\mathbf{F}_p = \begin{bmatrix} 3r_m^2 p_z^2 & 0 & -3r_m^2 p_x p_z \\ 0 & 3r_m^2 p_z^2 & -3r_m^2 p_y p_z \\ -3r_m^2 p_x p_z & -3r_m^2 p_y p_z & -3r_m^2\left(p_x^2 + p_y^2 + 2r_b^2 \sin^2\left(\dfrac{\varphi_m - \varphi_b}{2}\right)\right) \end{bmatrix} \tag{50}$$

$$\mathbf{F}_p^{\mathrm{T}}\mathbf{F}_o = \begin{bmatrix} 0 & -3r_m p_z k & 0 \\ 3r_m p_z k & 0 & 0 \\ -3r_m p_y k & 3r_m p_z k & 0 \end{bmatrix} \tag{51}$$

$$L = \sqrt{\frac{r_m^2\left(p_x^2 + p_y^2 + 2p_z^2 + 2r_b^2 \sin^2\left(\dfrac{\varphi_m - \varphi_b}{2}\right)\right)}{2\left(p_x^2 + p_y^2 + p_z^2 + \eta^2\right)}}. \tag{52}$$

Here, p_x, p_y and p_z are the components of the position vector $\mathbf{p}$ as defined in eq. (24) and η and k are written as

$$\eta = \sqrt{r_m^2 + r_b^2 - 2r_m r_b \cos\left(\frac{\varphi_m - \varphi_b}{2}\right)} \tag{53}$$

$$k = r_m - r_b \cos\left(\frac{\varphi_m - \varphi_b}{2}\right), \tag{54}$$

where η is the projection of each leg on the base platform. Using the isotropic conditions for matrix $\mathbf{A}$, namely, eqs. (26), the following results can be obtained

$$p_x = 0 \qquad p_y = 0 \tag{55}$$

$$r_m = r_b \cos\left(\frac{\varphi_m - \varphi_b}{2}\right). \tag{56}$$

Upon substituting eqs. (55) and (56) into eqs.(49)–(52) and using the values of η and k at isotropic condition, i.e., $\eta = r_b \sin\left(\frac{\varphi_m - \varphi_b}{2}\right)$ and $k = 0$, we obtain

$$\mathbf{F}_o^{\mathrm{T}}\mathbf{F}_o = \begin{bmatrix} 3\eta^2 & 0 & 0 \\ 0 & 3\eta^2 & 0 \\ 0 & 0 & 6p_z^2 \end{bmatrix} \tag{57}$$

$$\mathbf{F}_p^{\mathrm{T}}\mathbf{F}_p = \begin{bmatrix} 3r_m^2 p_z^2 & 0 & 0 \\ 0 & 3r_m^2 p_z^2 & 0 \\ 0 & 0 & 6r_m^2 \eta^2 \end{bmatrix} \tag{58}$$

$$\mathbf{F}_p^{\mathrm{T}}\mathbf{F}_o = \mathbf{0} \tag{59}$$

$$L = r_m. \tag{60}$$

Moreover, since the MP has only translational motion and in the light of eq. (55), we can show that the projections of each leg along the Z-axis are identical and equal to each other. This means that the angle of leg i with respect to the vertical axis for all legs is identical, i.e., $\beta_i = \beta$ for $i = 1, \ldots, 6$. Therefore, the lengths of the legs are equal to each other, namely, $q_i = q$ for $i = 1, \ldots, 6$. This makes matrix $\mathbf{B}$ have identical elements and hence matrix $\mathbf{B}$ is in the isotropic condition (Hasan Ghasemi 2000). Hence, η and p_z at the isotropic configuration can be written as

$$\eta = \sqrt{l_{ix}^2 + l_{iy}^2} = q \sin\beta \tag{61a}$$

$$p_z = l_{iz} = q \cos\beta, \tag{61b}$$

where l_{ix}, l_{iy} and l_{iz} are the components of $\mathbf{l}_i$, i.e., the position vector $\overrightarrow{B_i P_i}$ as shown in Figure 3. Upon substituting eqs. (55), (60), (61a) and (61b) into eqs. (57) and (58), we obtain

$$\mathbf{F}_o^{\mathrm{T}}\mathbf{F}_o = 3q^2 \begin{bmatrix} \sin^2\beta & 0 & 0 \\ 0 & \sin^2\beta & 0 \\ 0 & 0 & 2\cos^2\beta \end{bmatrix} \tag{62}$$

$$\frac{1}{L^2}\mathbf{F}_p^{\mathrm{T}}\mathbf{F}_p = 3q^2 \begin{bmatrix} \cos^2\beta & 0 & 0 \\ 0 & \cos^2\beta & 0 \\ 0 & 0 & 2\sin^2\beta \end{bmatrix}. \tag{63}$$

Matrix $\mathbf{F}_o$ is in the isotropic condition when the diagonal elements of matrix $\mathbf{F}_o^{\mathrm{T}}\mathbf{F}_o$ of eq. (62) are identical, namely,

$$\sin^2\beta = 2\cos^2\beta. \tag{64}$$

Here, $\beta = \pm\tan^{-1}(\sqrt{2})$ for the isotropic condition of matrix $\mathbf{F}_o$. Hence, $\mathrm{KCI}(\mathbf{F}_p) = 25\%$ when the matrix $\mathbf{F}_o$ is in the isotropic condition. Moreover, the diagonal elements of matrix $\mathbf{F}_p$ should also be identical to satisfy the isotropic condition for matrix $\mathbf{F}_p$, i.e.,

$$\cos^2\beta = 2\sin^2\beta. \tag{65}$$

Here, $\beta = \pm\tan^{-1}(\sqrt{2}/2)$ for the isotropic condition of matrix $\mathbf{F}_p$ which makes $\mathrm{KCI}(\mathbf{F}_o) = 25\%$. Therefore, eqs. (64) and (65) should hold simultaneously to have isotropic condition for both matrices $\mathbf{F}_o$ and $\mathbf{F}_p$. These two equations are nonlinear equations in terms of one unknown, i.e., β. There is no real solution for the equations and thus the approximate solution can be determined using the least-squares error method. The functions $\cos^2\beta - 2\sin^2\beta$ and $\sin^2\beta - 2\cos^2\beta$ versus β are shown in Figure 13. As shown, function $\cos^2\beta - 2\sin^2\beta$ vanishes at $\beta = 35.3°$ and function $\sin^2\beta - 2\cos^2\beta$ vanishes at $\beta = 54.7°$. The error function is chosen as

$$f = \sqrt{(\cos^2\beta - 2\sin^2\beta)^2 + (\sin^2\beta - 2\cos^2\beta)^2}. \tag{66}$$

The function f versus β is depicted in Figure 14. As shown in Figure 14, the function f has the minimum value at $\beta =$

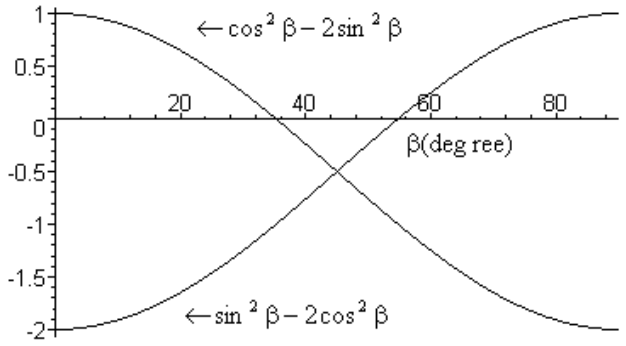

Fig. 13. Functions $\cos^2\beta - 2\sin^2\beta$ and $\sin^2\beta - 2\cos^2\beta$ versus β.

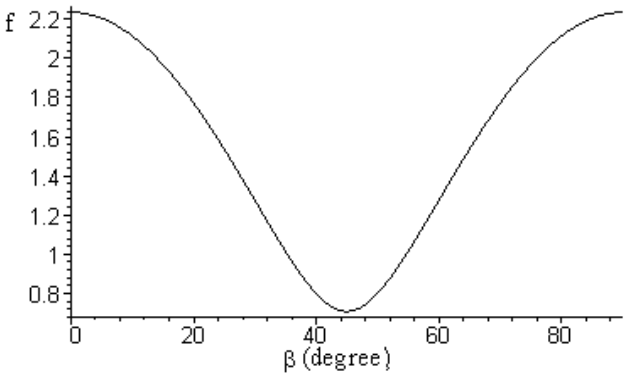

Fig. 14. The error function versus β.

45°. Upon using $\beta = 45°$ as an approximate solution for the isotropic condition of matrices $\mathbf{F}_o$ and $\mathbf{F}_p$, the diagonal elements of both $\mathbf{F}_o$ and $\mathbf{F}_p$ matrices become $\frac{3}{\sqrt{2}}$, $\frac{3}{\sqrt{2}}$ and $\frac{6}{\sqrt{2}}$, respectively. Therefore, the condition numbers of both $\mathbf{F}_o$ and $\mathbf{F}_p$ matrices are equal to $\sqrt{2}$, which results in KCI($\mathbf{F}_o$) = KCI($\mathbf{F}_p$) = 70.7%. Upon substituting $\beta = 45°$ into eq. (61a) and in light of $\eta = r_b \sin\left(\frac{\varphi_m - \varphi_b}{2}\right)$, the length of each leg at the isotropic configuration is derived as

$$q = \sqrt{2} r_b \sin\left(\frac{\varphi_m - \varphi_b}{2}\right). \tag{67}$$

The isotropic conditions for translational motion of the MP for the Stewart–Gough platform have been derived in this section. We have computed the conditions that are required for the isotropic condition. Nevertheless, some of these conditions have been assumed in a previous research work without deriving them (Zanganeh and Angeles 1997).

4. Numerical Method

The isotropic conditions for both manipulators are determined numerically by applying the conditions on matrix $\mathbf{G}$ of eq. (30).

In the isotropic design, the Jacobian matrix $\mathbf{G}$ has nonzero identical singular values or it has unit condition number. Therefore, matrices $\mathbf{G}\mathbf{G}^{\mathrm{T}}$ or $\mathbf{G}^{\mathrm{T}}\mathbf{G}$ become proportional to an identity matrix. The isotropy condition for matrix $\mathbf{G}$ can be written as

$$\mathbf{G}^{\mathrm{T}}\mathbf{G} = \alpha^2 \mathbf{I}, \tag{68}$$

where α is a scalar and $\mathbf{I}$ is an identity matrix. Upon substituting $\mathbf{G}$ from eq. (29) into eq. (68), we find

$$\mathbf{G}^{\mathrm{T}}\mathbf{G} = \mathbf{A}^{\mathrm{T}}(\mathbf{B}^{-1})^2\mathbf{A} = \alpha^2\mathbf{I}. \tag{69}$$

Here, we also use the characteristic length L in order to homogenize the elements of the Jacobian matrix to have the same dimension. Therefore, some of the columns are divided by a length L. Thus matrix $\mathbf{A}$ is divided into two submatrices as

$$\mathbf{A} = \begin{bmatrix} \frac{1}{L}\mathbf{F}_p & \mathbf{F}_o \end{bmatrix}. \tag{70}$$

Upon substituting $\mathbf{A}$ from eq. (70) into eq. (69), we obtain

$$\mathbf{G}^{\mathrm{T}}\mathbf{G} = \begin{bmatrix} \frac{1}{L^2}\mathbf{F}_p^{\mathrm{T}}(\mathbf{B}^{-1})^2\mathbf{F}_p & \frac{1}{L}\mathbf{F}_p^{\mathrm{T}}(\mathbf{B}^{-1})^2\mathbf{F}_o \\ \frac{1}{L}\mathbf{F}_o^{\mathrm{T}}(\mathbf{B}^{-1})^2\mathbf{F}_p & \mathbf{F}_o^{\mathrm{T}}(\mathbf{B}^{-1})^2\mathbf{F}_o \end{bmatrix} = \begin{bmatrix} \alpha^2\mathbf{I} & \mathbf{0} \\ \mathbf{0} & \alpha^2\mathbf{I} \end{bmatrix}. \tag{71}$$

The isotropic conditions for the 3-DoF manipulator are studied first, using numerical analysis.

4.1 The 3-DoF Spatial Parallel Manipulator

The matrices $\mathbf{F}_p$ and $\mathbf{F}_o$ of eq. (71) for this manipulator can be written as

$$\mathbf{F}_p = \begin{bmatrix} k1 & k2 \\ k3 & k4 \\ k5 & k6 \end{bmatrix} \quad \mathbf{F}_o = \begin{bmatrix} k7 \\ k8 \\ k9 \end{bmatrix}, \tag{72}$$

where the elements of matrices $\mathbf{F}_p$ and $\mathbf{F}_o$ are defined in the light of eq. (4) as

$$k1 = r_m(r_b \sin\varphi + h\cos\varphi) \tag{73a}$$

$$k2 = 0 \tag{73b}$$

$$k3 = -\sqrt{3}/4 r_m r_b \cos\varphi \sin\psi + 1/4 r_m r_b \sin\varphi - \sqrt{3}/2 r_m h \sin\varphi \sin\psi - 1/2 r_m h \cos\varphi \tag{73c}$$

$$k4 = 3/4 r_m r_b \sin\psi - \sqrt{3}/4 r_m r_b \sin\varphi\cos\psi + \sqrt{3}/2 r_m h \cos\varphi\cos\psi \quad (73d)$$

$$k5 = \sqrt{3}/4 r_m r_b \cos\varphi\sin\psi + 1/4 r_m r_b \sin\varphi + \sqrt{3}/2 r_m h \sin\varphi\sin\psi - 1/2 r_m h\cos\varphi \quad (73e)$$

$$k6 = 3/4 r_m r_b \sin\psi + \sqrt{3}/4 r_m r_b \sin\varphi\cos\psi - \sqrt{3}/2 r_m h\cos\varphi\cos\psi \quad (73f)$$

$$k7 = h + r_m \sin\varphi \quad (73g)$$

$$k8 = h + \sqrt{3}/2 r_m \cos\varphi\sin\psi - 1/2 r_m \sin\varphi \quad (73h)$$

$$k9 = h - \sqrt{3}/2 r_m \cos\varphi\sin\psi - 1/2 r_m \sin\varphi. \quad (73i)$$

The isotropic condition for this manipulator is written as

$$\mathbf{G}^{\mathrm{T}}\mathbf{G} = \alpha^2 \begin{bmatrix} \mathbf{I}_2 & \mathbf{0} \\ \mathbf{0} & 1 \end{bmatrix}, \quad (74)$$

where $\mathbf{I}_2$ is a 2×2 identity matrix.

Upon substituting eqs. (72) into eq. (74) and in the light of eq. (71), we obtain the isotropic conditions for the manipulator as

$$\frac{1}{L^2}\mathbf{F}_p^{\mathrm{T}}\mathbf{B}^{-2}\mathbf{F}_p = \alpha^2\mathbf{I}_2 \quad (75)$$

$$\mathbf{F}_o^{\mathrm{T}}\mathbf{B}^{-2}\mathbf{F}_o = \alpha^2 \quad (76)$$

$$\frac{1}{L}\mathbf{F}_p^{\mathrm{T}}\mathbf{B}^{-2}\mathbf{F}_o = \mathbf{0}. \quad (77)$$

The traces of both sides of eqs.(75) and (77) lead to

$$L^2 = \frac{\mathrm{tr}\left(\mathbf{F}_p^{\mathrm{T}}\mathbf{B}^{-2}\mathbf{F}_p\right)}{2\mathbf{F}_o^{\mathrm{T}}\mathbf{B}^{-2}\mathbf{F}_o}. \quad (78)$$

Upon substituting eqs. (73) into eqs. (75)–(78), we obtain an overdetermined system of equations with seven equations, namely, three equations related to eq. (75), one equation for eq. (76) and two equations for eq. (77) in four unknowns, namely, φ, ψ, h and L. The least- squares method is used to solve the set of equations numerically. The following physical parameters are used for the manipulator at hand. The moving platform side is 1 m, the base platform side is 2 m, and the values of a_i and b_i $(i = 1, 2, 3)$ are defined as

$$a_1 = \begin{bmatrix} 0 & 0.577 & 0 \end{bmatrix}^{\mathrm{T}} \quad (79)$$

$$a_2 = \begin{bmatrix} -0.5 & -0.289 & 0 \end{bmatrix}^{\mathrm{T}} \quad (80)$$

$$a_3 = \begin{bmatrix} 0.5 & -0.289 & 0 \end{bmatrix}^{\mathrm{T}} \quad (81)$$

$$b_1 = \begin{bmatrix} 0 & 1.155 & 0 \end{bmatrix}^{\mathrm{T}} \quad (82)$$

$$b_2 = \begin{bmatrix} -1 & -0.577 & 0 \end{bmatrix}^{\mathrm{T}} \quad (83)$$

$$b_3 = \begin{bmatrix} -1 & -0.577 & 0 \end{bmatrix}^{\mathrm{T}}. \quad (84)$$

Using the isotropic conditions and the numerical method explained in this section, we can obtain the following configuration for the isotropic design of the manipulator:

$$\begin{aligned} \varphi &= -25.78^\circ \\ \psi &= 0^\circ \\ h &= 0.09 \text{ m} \\ L &= 0.4324 \text{ m} \end{aligned} \quad (85)$$

It may be noted that solving overdetermined systems of equations using the least-squares method leads to approximate solutions. In other words, it is not possible to obtain the solution with a KCI of 100% for the matrix $\mathbf{G}$.

Next, we derive the isotropic conditions for the Stewart–Gough platform numerically.

4.2 Stewart–Gough Platform

The matrices $\mathbf{F}_p$ and $\mathbf{F}_o$ of eq. (70) for this manipulator can be written as

$$\mathbf{F}_p = \begin{bmatrix} (\mathbf{a}_1 \times \mathbf{l}_1)^{\mathrm{T}} \\ (\mathbf{a}_2 \times \mathbf{l}_2)^{\mathrm{T}} \\ (\mathbf{a}_3 \times \mathbf{l}_3)^{\mathrm{T}} \\ (\mathbf{a}_4 \times \mathbf{l}_4)^{\mathrm{T}} \\ (\mathbf{a}_5 \times \mathbf{l}_5)^{\mathrm{T}} \\ (\mathbf{a}_6 \times \mathbf{l}_6)^{\mathrm{T}} \end{bmatrix} \quad \mathbf{F}_o = \begin{bmatrix} \mathbf{l}_1^{\mathrm{T}} \\ \mathbf{l}_2^{\mathrm{T}} \\ \mathbf{l}_3^{\mathrm{T}} \\ \mathbf{l}_4^{\mathrm{T}} \\ \mathbf{l}_5^{\mathrm{T}} \\ \mathbf{l}_6^{\mathrm{T}} \end{bmatrix}. \quad (86)$$

The isotropic condition for the Stewart–Gough platform is written as

$$\mathbf{G}^{\mathrm{T}}\mathbf{G} = \alpha^2 \begin{bmatrix} \mathbf{I}_3 & \mathbf{0} \\ \mathbf{0} & \mathbf{I}_3 \end{bmatrix}, \quad (87)$$

where $\mathbf{I}_3$ is a 3×3 identity matrix.

Comparing eq. (86) with eq. (87) and in the light of eq. (71), we can obtain the isotropic conditions for the manipulator as

$$\frac{1}{L^2}\mathbf{F}_p^{\mathrm{T}}(\mathbf{B}^{-1})^2\mathbf{F}_p = \alpha^2\mathbf{I}_3 \quad (88)$$

$$\mathbf{F}_o^{\mathrm{T}}(\mathbf{B}^{-1})^2\mathbf{F}_o = \alpha^2\mathbf{I}_3 \quad (89)$$

$$\frac{1}{L}\mathbf{F}_p^{\mathrm{T}}(\mathbf{B}^{-1})^2\mathbf{F}_o = \mathbf{0}. \quad (90)$$

The traces of eqs.(88) and (89) lead us to

$$\alpha^2 = 2 \quad (91)$$

$$L^2 = \frac{1}{6}\sum_{i=1}^{6}\frac{\|\mathbf{m}_i\|^2}{q_i^2} \quad (92)$$

where q_i is length of the leg i and $\mathbf{m}_i$ is written as

$$\mathbf{m}_i = \mathbf{a}_i \times \mathbf{I}_i \quad (i = 1, \ldots, 6). \tag{93}$$

Equations (88), (89), (90) and (92) consist of a set of 22 equations in seven unknowns. We have twelve equations for the first two equations, i.e., eqs. (88) and (89), because of the symmetry matrix. There are nine equations for eq. (90) and one equation for eq. (92). The unknowns are the position vector components, i.e., (p_x, p_y, p_z), the fixed Euler angles namely (φ, ψ and θ) of the MP and the characteristic length L.

Therefore, we have an overdetermined system of equations that should be solved numerically. The least-squares method is used to solve this system of equations. One practical Stewart–Gough platform that is used as a moving mechanism in a flight simulator (CAE 500 Seri, CAE Electronics Inc., Canada; a typical model of a commerical flight simulator) is used as a numerical example to determine the isotropic conditions for the manipulator at hand. The physical and geometric parameters of the mechanism are as follows.

The base platform is a semi-hexagon with small sides of 0.1905 m and the larger sides of 3.3137 m. The radii of circumferential circle for the BP and MP are 1.97 m and 2.24 m, respectively. The MP is also a semi-hexagon with small sides of 0.5842 m and the larger sides of 3.5560 m. Therefore, the numerical values of the position vectors $\mathbf{a}_i$ and $\mathbf{b}_i$ ($i = 1, \ldots, 6$) defined in eqs.(5)–(16) for this example are written as

$$\mathbf{a}_1 = \begin{bmatrix} 1.3636 & -1.7771 & 0 \end{bmatrix}^{\mathrm{T}} \tag{94}$$

$$\mathbf{a}_2 = \begin{bmatrix} 1.3636 & 1.7771 & 0 \end{bmatrix}^{\mathrm{T}} \tag{95}$$

$$\mathbf{a}_3 = \begin{bmatrix} 0.8572 & 2.0965 & 0 \end{bmatrix}^{\mathrm{T}} \tag{96}$$

$$\mathbf{a}_4 = \begin{bmatrix} -2.2208 & 0.2924 & 0 \end{bmatrix}^{\mathrm{T}} \tag{97}$$

$$\mathbf{a}_5 = \begin{bmatrix} -2.2208 & -0.2924 & 0 \end{bmatrix}^{\mathrm{T}} \tag{98}$$

$$\mathbf{a}_6 = \begin{bmatrix} 0.8572 & -2.0695 & 0 \end{bmatrix}^{\mathrm{T}} \tag{99}$$

$$\mathbf{b}_1 = \begin{bmatrix} 1.9673 & -0.1031 & 0 \end{bmatrix}^{\mathrm{T}} \tag{100}$$

$$\mathbf{b}_2 = \begin{bmatrix} 1.9673 & 0.1031 & 0 \end{bmatrix}^{\mathrm{T}} \tag{101}$$

$$\mathbf{b}_3 = \begin{bmatrix} -0.8944 & 1.7552 & 0 \end{bmatrix}^{\mathrm{T}} \tag{102}$$

$$\mathbf{b}_4 = \begin{bmatrix} -1.0729 & 1.6521 & 0 \end{bmatrix}^{\mathrm{T}} \tag{103}$$

$$\mathbf{b}_5 = \begin{bmatrix} -1.0729 & -1.6521 & 0 \end{bmatrix}^{\mathrm{T}} \tag{104}$$

$$\mathbf{b}_6 = \begin{bmatrix} -0.8944 & -1.7552 & 0 \end{bmatrix}^{\mathrm{T}} \tag{105}$$

where all values are in meters.

Applying the isotropic conditions for this practical example and solving the overdetermined systems, it is possible to obtain the isotropic configuration of the mechanism as

$$\begin{aligned} &p_x = 0, \quad p_y = 0, \quad p_z = 2.06 \text{ m} \\ &\varphi = \psi = \theta = 0 \\ &L = 2.1. \end{aligned} \tag{106}$$

It may be noted that the least-squares method results in approximate solutions to overdetermined systems of equations. KCI($\mathbf{G}$) is 20.34% for this example and the lengths of the legs should be identical and equal to 2.06 m. Hence, this Stewart–Gough platform with the above-mentioned parameters is far from being isotropic. In other words, this is the best solution that we can derive using the least-squares method for the manipulator at hand with the specified geometric parameters.

5. Discussion of Results

The isotropic conditions for two spatial manipulators were studied using two different methods. The first method was based on the isotropic conditions of two Jacobian matrices, i.e., $\mathbf{A}$ and $\mathbf{B}$, instead of using only one Jacobian matrix, $\mathbf{G} = \mathbf{B}^{-1}\mathbf{A}$. Substituting the isotropic matrices $\mathbf{A}$ and $\mathbf{B}$ from eqs. (26) and (27) into $\mathbf{G}^{\mathrm{T}}\mathbf{G}$, we obtain

$$\begin{aligned} \mathbf{G}^{\mathrm{T}}\mathbf{G} &= \mathbf{A}^{\mathrm{T}}\mathbf{B}^{-\mathrm{T}}\mathbf{B}^{-1}\mathbf{A} = \mathbf{A}^{\mathrm{T}}(\mathbf{B}^{\mathrm{T}}\mathbf{B})^{-1}\mathbf{A} \\ &= \mathbf{A}^{\mathrm{T}}(\tau^2\mathbf{I})^{-1}\mathbf{A} = \frac{1}{\tau^2}\sigma^2\mathbf{I} = \alpha^2\mathbf{I}. \end{aligned} \tag{107}$$

As shown, $\mathbf{G}^{\mathrm{T}}\mathbf{G}$ is proportional to an identity matrix. Hence, if the matrices $\mathbf{A}$ and $\mathbf{B}$ are isotropic, then matrix $\mathbf{G}$ is also isotropic. On the other hand, if matrices $\mathbf{A}$ and $\mathbf{B}$ are not isotropic, then the following expression can be written for the condition numbers of these matrices and matrix $\mathbf{G}$: $k(\mathbf{G}) \leq k(\mathbf{B})k(\mathbf{A})$. Hence, by decreasing the condition numbers or increasing the KCI of $\mathbf{A}$ and $\mathbf{B}$, the condition number of $\mathbf{G}$ will also decrease, which results in an increase of KCI ($\mathbf{G}$).

We have used the isotropic conditions on both matrices $\mathbf{A}$ and $\mathbf{B}$ in Section 3 because it is very cumbersome to study the isotropic conditions for matrix $\mathbf{G}$ symbolically.

However, the second method based on isotropic conditions on matrix $\mathbf{G}$ was used for numerical computations in Section 4.

6. Conclusion

We have presented a study of the isotropic design of two spatial parallel manipulators, one with 3-DoF and the other with 6-DoF. The isotropic design of the 3-DoF manipulator was studied first. The kinematic constraint equation of the manipulator was determined symbolically. Although the isotropic solution, obtained from the equations, is mathematically acceptable, it is an impossible configuration from a physical point of view. In other words, we could not obtain a solution for the isotropic design of the manipulator with a KCI

of 100%. Therefore, the isotropic solutions were modified by changing the height or heave of the manipulator so as to obtain a desired KCI. The variations of KCI with respect to the roll and pitch angles of the MP are determined in order to present a nearly isotropic design for the manipulator at hand.

Next, the isotropic design of the Stewart–Gough platform was studied. Since the kinematic constraint equations are very cumbersome and the number of variables is large, it is hardly possible to obtain the isotropic condition symbolically for a general motion of the MP. Thus the isotropic design was studied symbolically only for a general translational motion of the MP. It may be noted that it is not possible to obtain a KCI of 100% even for this motion. Eventually the isotropic conditions for both manipulators were computed numerically using the least-squares method. This method gave approximate solutions for the isotropic configurations of both manipulators.

Acknowledgments

This work was made possible by financial support from Isfahan University of Technology. The authors would like to thank Dr Sunil Agrawal for his valuable comments.

References

Angeles, J. 1997. *Fundamentals of Robotics Mechanical Systems*. New York: Springer.

Angeles, J., and Lopez-Cajun, C. S. 1992. Kinematic isotropy and the conditioning index of serial type robotic manipulators. *International Journal of Robotics Research* 11(6):560–571.

Baron, L., and Bernier, G. 2001. The design of parallel manipulators of star topology under isotropic constraint. *Proc. ASME Design Engineering Technical Conferences*, Pittsburg, Pennsylvania, USA.

Carretero, J. A., Ron, P., Podhorodeski, R. P., Nahon, M. A., and Gosselin C. M. 2000. Kinematic analysis and optimization of a new three-degree-of-freedom spatial parallel manipulator. *ASME Journal of Mechanical Design*, 122(1):17–24.

Chablat, D., Wenger, P., and Angeles, J. 1998. The isoconditioning loci of a class of closed-chain manipulators. *Proc. IEEE International Conference on Robotics and Automation*, Leuven, pp. 1970–1975.

Fattah, A., and Oghbaei, M. 2000. Singular configurations and workspace of a parallel manipulator with new architecture. *Proc. ASME Design Engineering Technical Conferences*, Baltimore, MD, DETC2000/MECH-14100.

Gallant, M., and Boudreau, R. 2002. The synthesis of planar parallel manipulators with prismatic joints for an optimal, singularity-free workspace. *Journal of Robotic Systems*, 19(1):13–24.

Gosselin, C. M., and Angeles, J. 1988. The optimum kinematic design of a planar three-degree-of-freedom parallel manipulators. *Journal of Mechanisms, Transmissions, and Automation in Design*, 110(1):35–41.

Gosselin, C. M., and Lavoie, E. 1993. On the kinematic design of spherical three-degree-of-freedom parallel manipulators. *International Journal of Robotics Research* 12(4):394–402.

Gosselin, C. M., St-Pierre, E., and Gagné, M. 1996. On the development of the agile eye: mechanical design, control issues and experimentation. *IEEE Robotics and Automation Society Magazine* 3(4):29–37.

Hasan Ghasemi, M. 2000. Isotropic design of parallel manipulators. M.Sc. thesis, Isfahan University of Technology.

Huang, T., and Whitehouse, D. 1998. Local dexterity, optimal architecture and optimal design of parallel machine tools. *Annals of the CIRP* 47(1):347–351.

Mohammadi Daniali, H. R., and Zsombor-Murray, P. J. 1994. The design of isotropic planar parallel painpulators. In *Intelligent Automation and Soft Computing*, M. Jamshidi, J. Yuh, C.C. Nguyen, and R. Lumia, eds. Albuquerque, NM: TSI Press. Vol. 2, pp. 273–280.

Stewart, D. 1965. A platform with six degrees of freedom. *Proc. Inst. Mech. Eng.* 180,1(15):371–386.

Zanganeh, K. E., and Angeles, J. 1997. Kinematic isotropy and the optimum design of parallel manipulators. *International Journal of Robotic Research* 16(2):85–197.